SIEVE TRAY PRESSURE DROP BY MEANS OF CFD MODELING AND SIMULATION

Getye Gesit

School of Chemical and Bio Engineering, Addis Ababa Institute of Technology,
Addis Ababa University, Addis Ababa, Ethiopia
E-mail: getye.gesit@aait.edu.et

ABSTRACT

Sieve trays must be designed to have and operated at acceptably low enough tray pressure drop. Both of these tasks (i.e., tray design and tray analysis) require method(s) for sieve tray pressure drop determination. So far, only empirical correlations have been used for sieve tray pressure drop estimation. However, the correlations are not based on actual mechanics of flow but are based on gross oversimplifications and empirical correlations– hence often have large errors and are not reliable. A reliable and accurate way for the pressure drop determination can be achieved by use of working computational fluid dynamics (CFD) modeling and simulation. With working CFD model provided, the CFD modeling and simulation is mechanistic and first principles based or fundamentals based. In this work, a CFD model is developed and used to model and simulate and predict sieve tray pressure drop. The model considers the three-dimensional two-phase flow of gas (or vapour) and liquid in which each phase is treated as an interpenetrating continuum having separate transport equations. Interaction between the two phases occurs via interphase momentum transfer. For the CFD analysis, the commercial package CFX 17.0 of ANSYS was employed. Total and dry tray pressure drops are predicted for various combinations of gas and liquid flow rates. Predicted results are inacceptable and good agreement with experimental results.

The objective of the work was developing CFD model for sieve tray pressure drop and studying and finding out the extent to which the CFD modeling and simulation can be used as a prediction and design tool and method for sieve tray pressure drop. From the results and the CFD model performance, it is concluded that the CFD model provided here is acceptably good for sieve tray pressure drop modeling and simulation and hence is acceptably good for tray design and analysis.

Keywords: Sieve Tray, Pressure Drop, Tray Pressure Drop, Tray Design and Analysis, CFD Modeling and Simulation

INTRODUCTION

Sieve trays are widely used as phase contacting devices. They are commonly used in distillation that is the dominant separation process of the chemical and related processing industries. They are also used in the closely related mass transfer operations of absorption and stripping as well as in liquid-liquid extraction. Low cost, high separation efficiency, simplicity of fabrication and non-proprietary nature are some of the reasons that make sieve trays the first choice and standard column internals. Sieve tray design information may also be extended to the design of other type of trays.

Sieve trays must be designed to have and operated at acceptably low enough tray pressure drop. Both of these tasks (i.e., tray design and tray analysis) require method(s) for sieve tray pressure drop determination. So far, only empirical correlations have been used for sieve tray pressure drop estimation. However, the correlations are not based on actual mechanics of flow but are based on gross oversimplifications and empirical correlations– hence often have large errors and are not reliable.

Therefore, better models and methods of modeling and predicting sieve tray hydrodynamics and determining sieve tray pressure drop are of paramount significance and in dire need.

Recently, the development of powerful computers, advances in numerical methods, and improvements in multiphase flow models permit the investigation of complex flow problems. The technique that combines these is computational fluid dynamics (CFD), a technique that is emerging as an important predictive and design tool for flows in process equipment. Solution of the momentum, mass and energy transfer equations gives for each phase the time and spatial distribution fields of velocities, temperatures, pressures, volume fractions, and concentrations or compositions such as mole or mass fractions of species or components. The concern of this work is pressure drop determination. From the pressure solution distribution field of the CFD model and simulation, pressure drop can be calculated.

No CFD work has been done so far that is solely devoted to sieve tray pressure drop alone. There are no direct attempts made to use CFD for sieve tray pressure drop modeling and simulation Noriler, D, whose work was devoted to prediction of efficiencies, only briefly and partially mentions the prediction of tray pressure drop using CFD. [2], [3] whose works were devoted to prediction of weeping by CFD technique, present comparison of experimental and CFD prediction of sieve tray dry pressure drop. Therefore, so far there no works done that can be used to know first what models to use and second if CFD technique can be used for sieve tray pressure drop modeling and simulation.

The work of this paper is the only first work that presents and answers first what models to use and second if CFD technique can be used for sieve tray pressure drop modeling and simulation. In the work here, a CFD model is presented to model, simulate and predict the hydrodynamics and total and dry pressure drops of sieve trays. This work here studies, answers and presents modeling issues such as what flow geometry model to use, what mathematical model equations to use, what closure relations to use, there is a need to include the tray thickness, and what boundary conditions models to use. Tray geometry and fluids are based on the work of [4].

The CFD simulation results are inacceptable and good agreement with the experimental results of Thomas. The objective of this work was developing CFD model and studying and finding out the extent to which the CFD modeling and simulation can be used as a modeling and simulation and prediction tool and method for pressure drop of sieve trays. From the results and the CFD model performance, it is concluded that the CFD model provided here is acceptably good for sieve tray pressure drop modeling and simulation and hence is acceptably good for tray design and analysis.

MODEL EQUATIONS

The model considers the flow of gas (or vapour) and liquid in the Eulerian-Eulerian framework in which each phase is treated as an interpenetrating continuum having separate transport equations. With the model focusing on the liquid-continuous region of the sieve tray as done in [5,6], the gas phase is taken as the dispersed phase and the liquid phase as the continuous phase. Since the focus is on the pressure drop behaviour of sieve trays, energy transfer has not been considered in this work since that has little or no effect on tray pressure drop simulations since the flow is essentially isothermal and incompressible. Thus for each phase the time and volume averaged continuity and momentum equations were numerically solved.

Continuity Equations

Gas phase

$$\frac{\partial}{\partial t}(r_G\rho_G) + \nabla.(r_G\rho_G\boldsymbol{V}_G) = 0 \qquad (1)$$

Liquid phase

$$\frac{\partial}{\partial t}(r_L\rho_L) + \nabla.(r_L\rho_L\boldsymbol{V}_L) = 0 \qquad (2)$$

Momentum Equations

Gas phase

$$\boldsymbol{\frac{\partial}{\partial t}(r_G\rho_G V_G) + \nabla.(r_G\rho_G V_G V_G) = -r_G\nabla p_G + \nabla.\left[r_G\mu_{eff,G}(\nabla V_G + (\nabla V_G)^T)\right] + r_G\rho_G g - M_{LG}} \qquad (3)$$

Liquid phase

$$\boldsymbol{\frac{\partial}{\partial t}(r_L\rho_L V_L) + \nabla.(r_L\rho_L V_L V_L) = -r_L\nabla p_L + \nabla.\left[r_L\mu_{eff,L}(\nabla V_L + (\nabla V_L)^T)\right] + r_L\rho_L g + M_{LG}} \qquad (4)$$

Equations (1) to (4) are for the unsteady state case. For the steady state case, terms involving the time derivative are zero. As one source for the equations, the ANSYS CFX 17.0 Documentation *ANSYS CFX* [7] can be consulted.

The gas and liquid volume fractions, r_G and r_L , are related by the summation constraint:

$$r_G + r_L = 1 \qquad (5)$$

The same pressure field has been assumed for both phases, i.e.,

$$p_G = p_L \qquad (6)$$

$\mu_{eff,G}$ and $\mu_{eff,L}$ are the effective viscosities of the gas and liquid phase, respectively, obtained as:

$$\mu_{eff,G} = \mu_{laminar,G} + \mu_{turbulent,G} \qquad (7)$$

$$\mu_{eff,L} = \mu_{laminar,L} + \mu_{turbulent,L} \qquad (8)$$

The term M_{LG} in the momentum equations represents interphase momentum transfer between the two phases.

Closure Relationships

In order to solve Equations (1) to (8) for velocities, pressure, and volume fractions, we need additional equations that relate the interphase momentum transfer term M_{LG} and the turbulent viscosities to the mean flow variables.

The interphase momentum transfer term M_{LG} is basically interphase drag force per unit volume. With the gas as the dispersed phase, the equation for M_{LG} is [7]:

$$M_{LG} = \frac{3}{4}\frac{C_D}{d_B} r_G\rho_L|V_G - V_L|(V_G - V_L) \qquad (9)$$

The interphase drag relation proposed by [8] was used. For the relation proposed by [8], the interphase momentum transfer term as a function of local variables and constant coefficients put in a form suitable for the CFD is:

$$M_{LG} = \frac{(r_G^{average})^2}{(1-r_G^{average})V_S^2} g(\rho_L - \rho_G) r_G r_L |V_G - V_L|(V_G - V_L) \quad (10)$$

For the average gas holdup fraction, $r_G^{average}$, the correlation of Bennett et al. [5] was used:

$$r_G^{average} = 1 - exp\left[-12.55\left(V_S\sqrt{\frac{\rho_G}{\rho_L-\rho_G}}\right)^{0.91}\right] \quad (11)$$

For the liquid and gas phase turbulence viscosities, a homogeneous shear stress transport turbulence model was selected and used. For turbulence transfer, Sato enhanced eddy viscosity model was also selected and used.

MODEL FLOW GEOMETRIES

The model sieve tray geometries were selected based on the work of Thomas. A round (or circular) and a rectangular cross-section sieve trays were modeled and simulated. This work studied the effect of tray geometry modeling. The geometry modeling issues investigated were whether to use one tray or two trays and whether to include or ignore the tray thickness. The study showed that unless two trays with tray thickness included are used, the CFD simulations will not predict the correct pressure drop. Inclusion of inlet down comer was also found to help convergence and hence was used. Of course, the right way is to use actual experimental sieve tray geometries and compare the results of experiments and CFD modeling and simulations, which is what is attempted in this work.

Details of the dimensions of the sieve trays are given in [4]. Just to give a view of the sizes of the trays, the circular one has a diameter of 0.8128 m and a tray spacing of 1.016 m while the rectangular one has an overall length of 0.9144 m, a width of 0.3048 m, and a tray spacing of 0.6096 m. Dimensions not present in Thomas need to be given and they are as follows. The down comer clearance height was set using the recommendations and relations found in Lieberman, N.P et al., and a down comer clearance of 63.5 mm was used for both the circular and rectangular cross-section sieve trays. For both trays, liquid (water) entrances are at the top of the tray horizontally in the negative x-axis direction 0.0762 m (equal to weir height) above the gas outlet holes plane. The heights of the liquid entrance used were 0.03 m for the circular sieve tray and 0.043175 m for the rectangular sieve tray. Liquid weir crest height relation found in Towler, G. was used for setting the heights of the liquid entrances.

For the circular cross-section sieve tray, symmetry was assumed about the centerline geometrical symmetry vertical plane and only half of the tray was considered so as to reduce computational load. For the rectangular cross-section sieve tray, the full tray was considered since it was possible to do so from computational load view point. For both shapes of trays, actual number and shape of holes were modeled since that was manageable. The whole tray spacing was considered in the simulation, even though the primary focus is in the froth region. This resulted in better numerical convergence, as well as provided with the ability to calculate tray pressure drops. The model sieve tray geometries and boundaries are shown in Figures 1 and 2.

MODEL BOUNDARY CONDITIONS

To solve the continuity and momentum equations, appropriate boundary conditions must be specified at all external boundaries plus at any specific internal boundaries of the flow geometry.

Boundary conditions were specified in line with that used in Gesit, G [12].

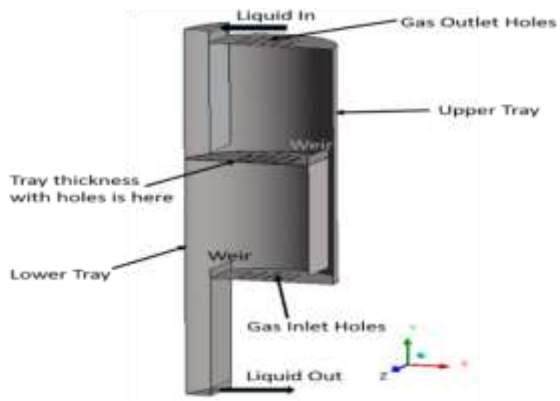

Figure 1 Model geometry and boundaries of the circular cross-section sieve tray (the plane of symmetry is just the whole front face of geometry shown, towards +z direction shown)

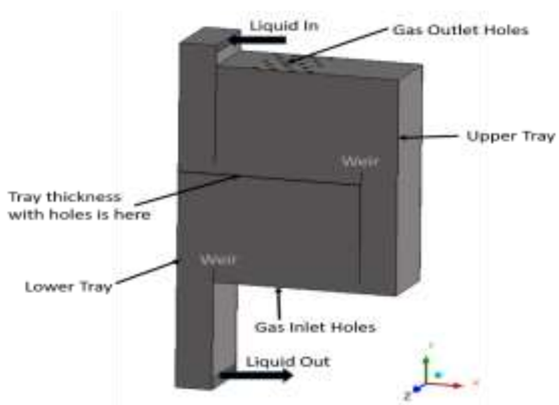

Figure 2 Model geometry and boundaries of the rectangular cross-section sieve tray (internal features are not visible and shown)

Liquid Inlet

For all simulations, uniform or flat inlet liquid velocity profile was specified. The liquid volume fraction at the liquid inlet was taken to be unity assuming that only liquid enters through the down comer clearance.

Gas Inlet

Uniform gas bubbling was used. The gas volume fraction at the inlet holes was specified to be unity.

Liquid and Gas Outlets

The liquid and gas outlet boundaries were specified as outlet boundaries with velocity specifications. At the liquid outlet, only liquid was assumed to leave the flow geometry and only gas was assumed to exit through the gas outlet. These specifications will be in agreement with the specifications at the gas inlet and liquid inlet where only one fluid phase was assumed to enter.

Wall and Symmetry Boundaries

The no-slip wall boundary condition was used for both the gas and liquid phases. The symmetry plane was specified as a symmetry boundary.

Operating conditions and system properties

Steady state CFD simulations were conducted for all modeling and simulations. The fluid system and operating conditions were based on the work of Thomas, so that comparisons could be made. The fluid system is air-water with both fluids and tray operation at 1 atmosphere pressure and room temperature (25 ^{o}C).

Mesh, mesh convergence and solution algorithms

Analysis Meshing 17.0 was used where default meshing method was used (which is Automatic: Patch Conforming/Sweeping), Physics was set to CFD and the Solver Preference was set to CFX. The number of nodes of the mesh has been given below. The meshing technology used is acceptable and the mesher tells if there is any unacceptable mesh statistics and if there is any mesh problem. For the meshes used here, the mesher didn't report any mesh problem and it also didn't report any unacceptable mesh statistics. Knowing the mesher used and the number of nodes, one can get the mesh statistics from the meshing software.

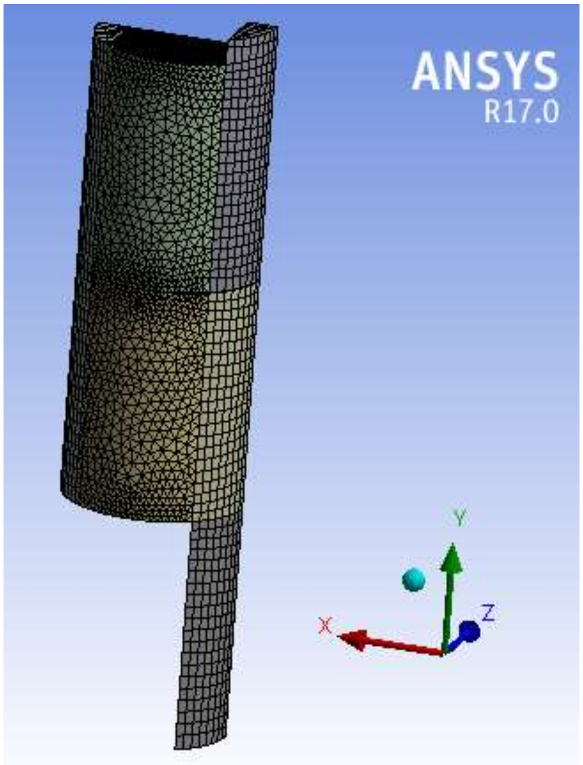

Figure 3 Mesh of circular cross-section sieve tray model geometry

The size of the mesh will have effect on the simulation results. Mesh size convergence study was conducted for the circular sieve tray. For the circular tray, above about 107087 nodes, the mesh size was found to have little effect on the simulation results and 107087 nodes mesh was selected as the working mesh. The rectangular sieve tray mesh was set at about the same mesh size of the circular one and 103819 nodes of mesh was selected as the working mesh. Table 1 gives the mesh convergence study CFD simulation results for the circular tray while Figures 3 and 4 show the meshed circular and rectangular sieve trays.

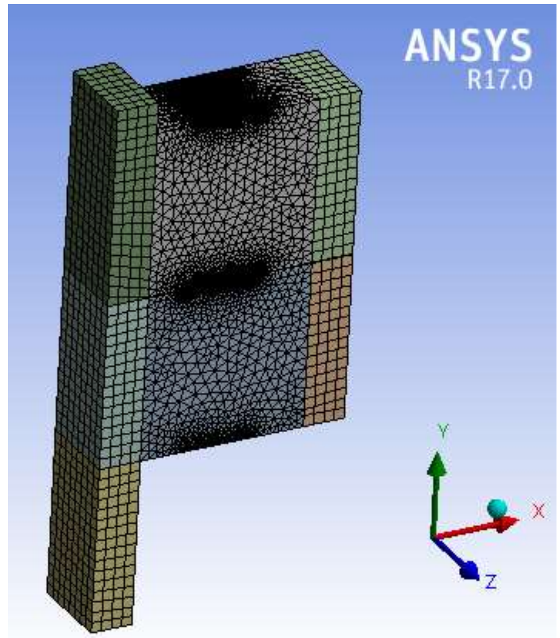

Figure 4 Mesh of rectangular cross-section sieve tray model geometry

Table 1 Mesh convergence study for the circular cross-section sieve tray (water flow rate = 2.27×10^{-3} m^3/s, air hole velocity = 14.78 m/s).

Number of Nodes of Mesh	Total Pressure Drop by CFD [Pa]
84265	691.359
107087	865.391
130300	869.727

High Resolution differencing scheme was used for all the equations. Convergence criteria of RMS = 10^{-5} was used for all simulations (default convergence criteria is RMS = 10^{-4})

One peculiar solution algorithm that needs to be mentioned is that volume fraction coupling was selected and initial volume fraction smoothing was set to volume-weighted and these resulted in better and faster convergence. All other algorithms are obvious from the models used here and elsewhere and while all others are default ones and need no mentioning.

Simulation Results

The ability of the CFD model and simulations to model, simulates, and predicts sieve tray pressure drop behaviour has been checked by calculating sieve tray pressure drop from the pressure solution field. The CFD model predicted total and dry sieve tray pressure drops are compared with the experimental results of Thomas, W.J and the results are presented in this section. The pressure drop was calculated from the pressure solution field as the area average of absolute pressure at the holes inlet at the bottom of the tray thickness (located at the middle in Figures 1 and 2) minus the area average of absolute pressure at the holes outlet at the top of the tray.

As shown in the graphs in this section, the CFD simulation results are inacceptable and good agreement with the experimental results of Thomas, W.J. The CFD model performance is acceptably good. Besides, the results of the CFD simulations exhibit the correct trend with respect to gas and liquid flow rates; i.e., the CFD simulation results correctly predict that pressure drop increases with either gas or liquid flow rate.

Results for the Circular (or Round) Sieve Tray

The total and dry sieve tray pressure drops of the CFD simulations results for the circular tray are shown in Figures 5 to 6. Figure 5 shows the total sieve tray pressure drop CFD simulation results whereas Figure 6 shows the dry sieve tray pressure drop CFD simulation results. Also shown and given in all Figures are the experimental results of Thomas, W.J

As shown in Figure 5, the CFD simulation results for the circular sieve tray total pressure drop are inacceptable and good agreement with the experimental results of Thomas, W.J. This good agreement implies that the CFD model provided by this work performed and worked well. The good agreement and good performance of the CFD model provided may be ascribed to the fact that the CFD model involves several aspects of mechanistic modeling. The fact that the CFD model is mechanistic and worked well makes it more reliable than empirical correlations. It can be stated that for all cases (both circular and rectangular trays) the CFD model performance is acceptably good

.

As shown in Figure 6, is shown the dry sieve tray pressure drop prediction of the CFD model compared with the experimental results of Thomas, W.J. The agreement between the CFD model results and the experiments can be stated as acceptably good. For the dry case, we have a single phase fluid flow (here only flow of air). Again, the CFD model involves several aspects of mechanistic modeling and works for the single phase flow too, and is hence more reliable than correlations.

Results for the Rectangular Sieve Tray

The total and dry sieve tray pressure drops results of the CFD simulations for the rectangular tray are shown in Figures 7 to 8. Figure 7 shows the total sieve tray pressure

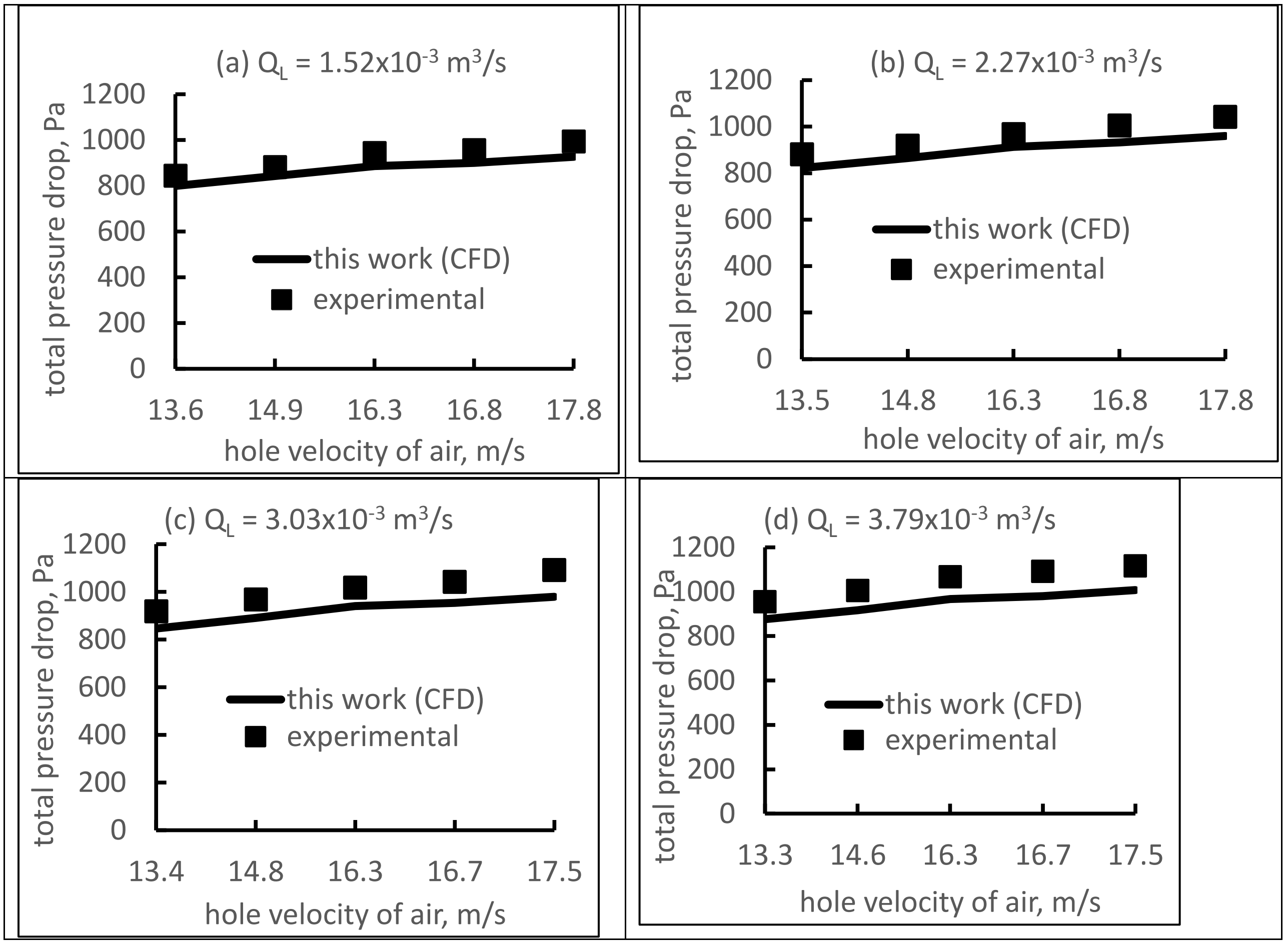

Figure 5 Total pressure drop of circular cross-section sieve tray

Drop CFD simulation results whereas Figure 8 shows the dry sieve tray pressure drop CFD simulation results. Also shown and given in all Figures are the experimental results of Thomas, W. J .

As shown in Figure 7, the CFD simulation results for the rectangular sieve tray total pressure drop are inacceptable and good agreement with the experimental results of Thomas, W. J For the rectangular sieve tray too, the CFD model has several mechanistic aspects of modeling and acceptably and reliably captured the flow behaviour and is hence more reliable than correlations.

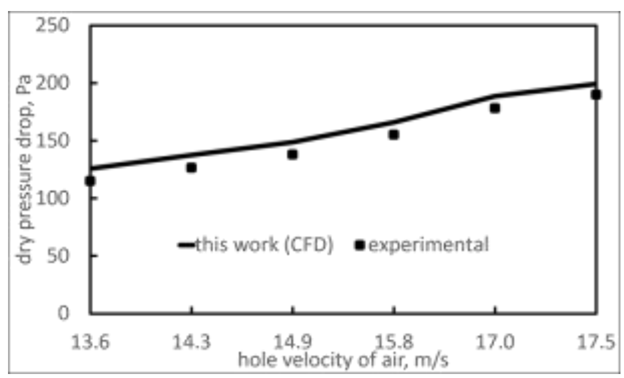

Figure 6 Dry pressure drop of circular cross-section sieve tray

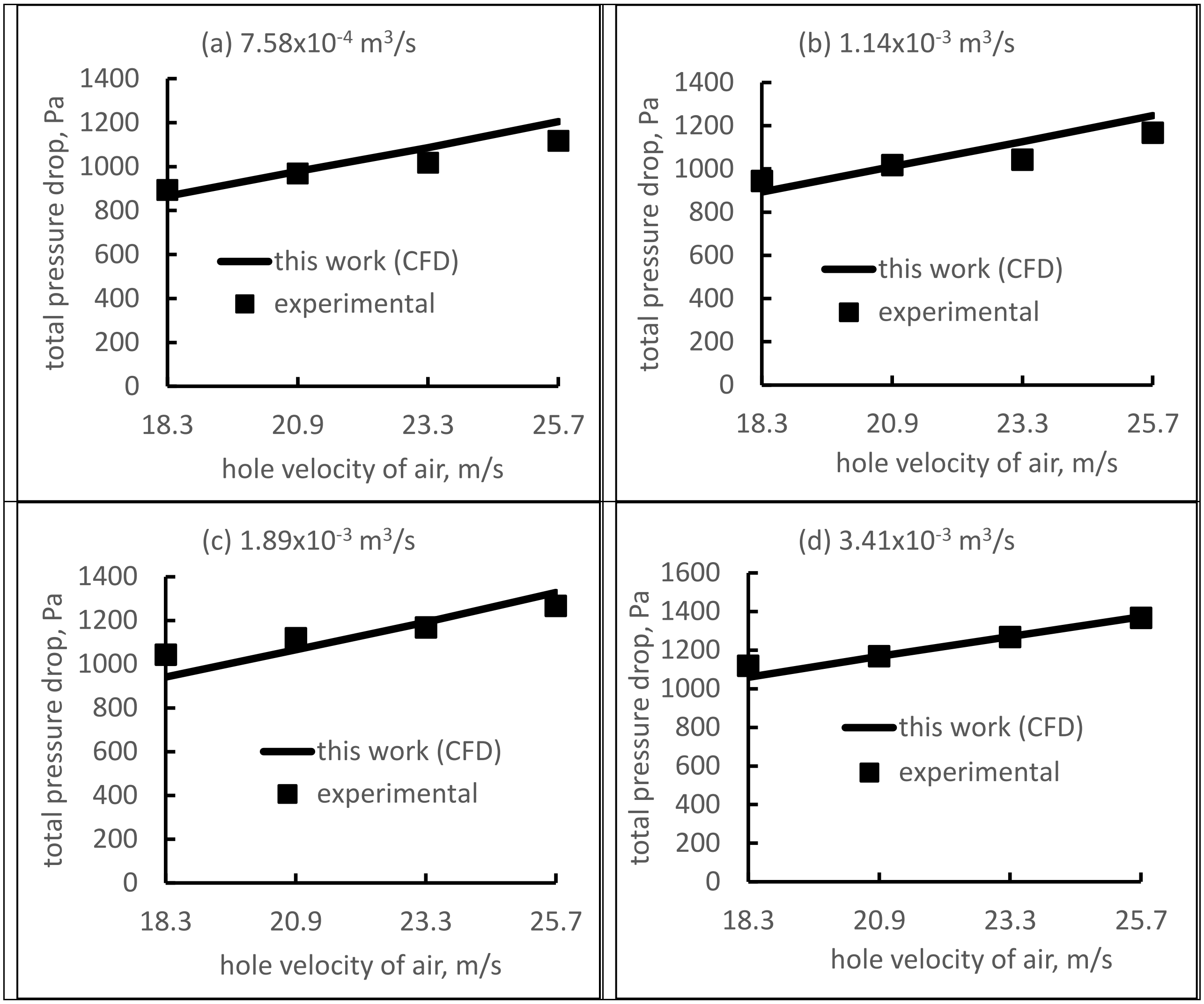

Figure 7 Total pressure drop of rectangular cross-section sieve tray

Figure 8 shows the dry pressure drop CFD model simulation results for the rectangular tray. It can be seen that the CFD model simulation results under predicted the dry pressure drop particularly at high gas rates.

The reason for this was found to be that some fraction of the gas bypassed the holes by going up through the lower down comer clearance. What is meant by this is depicted and explained by the gas streamlines shown in Figure 9 for the dry gas flow.

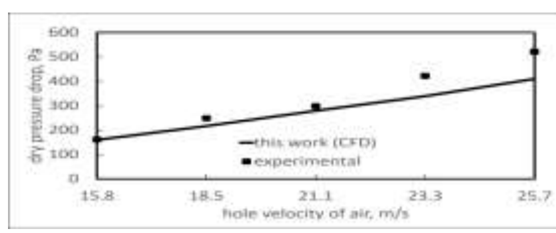

Figure 8 Dry pressure drop of rectangular cross-section sieve tray

But the gas streamlines of Figure 10, which are for the two phase flow case, show that there is little or no gas bypassing when two phase flow. The streamlines show the path followed by the gas.

A solution to this problem of gas bypassing holes is to use a model geometry that has gas inlet located above the lower down comer clearance. This will make all the gas pass through the holes.

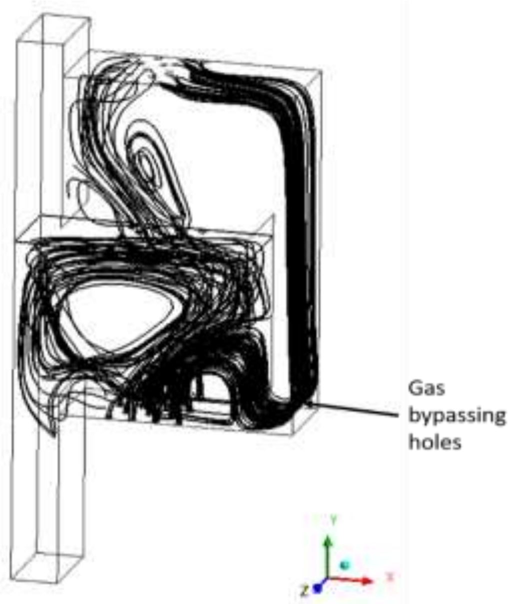

Figure 9 Gas streamlines (in dark black) of the single phase (dry gas) flow (air hole velocity = 25.7 m/s, rectangular tray)

CONCLUSIONS

This work provided validated model for modeling and simulating and predicting the pressure drop of sieve trays by means of computational fluid dynamics (CFD) using steady state simulations. The flow inside the tray was modeled as a three-dimensional two-phase flow of gas and liquid in the Eulerian-Eulerian framework. The time and volume averaged continuity and momentum transfer equations were numerically solved using the commercial package CFX 17.0 of ANSYS. The gas and liquid phase equations were coupled through appropriate interphase

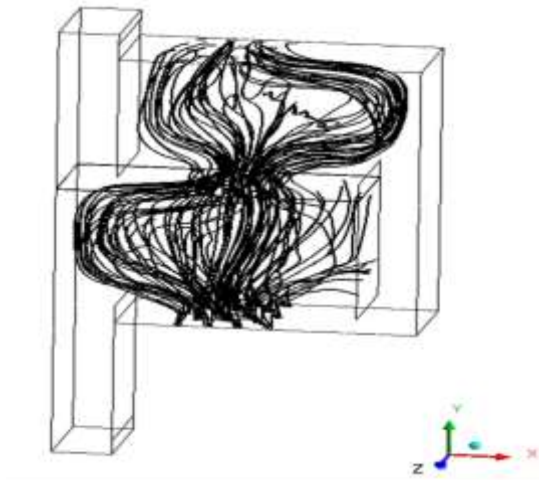

Figure 10 Gas streamlines (in dark black) of the two phase flow (water flow rate = $3.41\text{x}10^{-3}$ m^3/s, air hole velocity = 25.7 m/s, rectangular tray)

Momentum transfer closure model. Appropriate working CFD flow geometry model was also identified and provided. The CFD model was used to predict total and dry tray pressure drops. The CFD simulation results are inacceptable and good agreement with experimental results.

So far, only empirical correlations have been used to estimate sieve tray pressure drop. However, the correlations are not based on actual mechanics of flow but are based on gross oversimplifications and empirical correlations–hence often have large errors and are not reliable. Therefore, so far methods for satisfactorily modeling and predicting sieve tray pressure drop are lacking. This work showed that the CFD model provided here can be used as an acceptably good and a powerful tool and method for modeling and predicting sieve tray hydrodynamics and calculating tray pressure drop.

Compared to existing methods, the CFD model provides and adds appreciable good, significant, and advanced improvements and performance for sieve tray pressure drop determination. On top of being mechanistic, the modeling using CFD offers several advantages. For example, it overcomes many of the limitations associated with experiments and correlations and offers ease of changing tray geometry and operating conditions without incurring appreciable cost of time and other resources. From the results and the CFD model performance, it is concluded that the CFD model provided here is acceptably good for sieve tray pressure drop modeling and simulation and hence is acceptably good for tray design and analysis.

Nomenclature

C_D drag coefficient
d_B bubble diameter [m]
g gravitational acceleration vector [m s^{-2}]
g gravitational acceleration [m s^{-2}]
$\mathbf{M}_{LG}$ Interphase momentum transfer vector [kg m^{-2} s^{-2}]
p_G gas phase pressure [N m^{-2}]
p_L liquid phase pressure [N m^{-2}]
Q_L liquid volumetric flow rate [m^3/s]
r_G gas (or vapour) phase volume fraction
$r_G^{average}$ average gas holdup fraction in froth
r_L liquid phase volume fraction
V_G gas phase velocity vector [m/s]
V_L liquid phase velocity vector [m/s]
V_S gas phase superficial velocity based on bubbling area [m/s]

Greek Letters

$\mu_{laminar,G}$ molecular viscosity of gas [kg m^{-1} s^{-1}]
$\mu_{laminar,L}$ molecular viscosity of liquid [kg m^{-1} s^{-1}]
$\mu_{turbulent,G}$ turbulent viscosity of gas [kg m^{-1} s^{-1}]
$\mu_{turbulent,L}$ turbulent viscosity of liquid [kg m^{-1} s^{-1}]
$\boldsymbol{\rho_G}$ gas phase mass density [kg/m^3]
$\boldsymbol{\rho_L}$ liquid phase mass density [kg/m^3]

REFERENCES

[1] Noriler, D., Barros, A.A.C., Maciel, .R.W., and Meier, H.F., "*Simultaneous Momentum, Mass, and Energy Transfer Analysis of a Distillation Sieve Tray using CFD Techniques: Prediction of Efficiencies*", Ind. Eng. Chem. Res., Vol. 49, 2010, pp. 6599–6611.

[2] Zarei, A., Hosseini, S.H., and Rahimi, R.,"*CFD and experimental studies of liquid weeping in the circular sieve tray columns*", Chemical Engineering Research and Design, Vol. 91, No. 12, 2013, pp. 2333-2345.

[3] Zarei, A., Hosseini, S.H., and Rahimi, R., "*CFD study of weeping rate in the rectangular sieve tray columns*", Journal of the Taiwan Institute of Chemical Engineers, Vol. 44, 2013, pp. 27-33.

[4] Thomas, W.J. and Ogboja, O., "*Hydraulic Studies in Sieve Tray Columns*", Ind. Eng. Chem. Process Des. Dev., Vol. 17, No. 4, 1978, pp. 429-443.

[5] Bennett, D. L., Agrawal, R. and Cook, P. J., "*New Pressure Drop Correlation for Sieve Tray Distillation Columns*", AIChE Journal, Vol. 29, 1983, pp. 434-442.

[6] Bennett, D.L., Watson, D.N. and Wiescinski, M.A., "*New Correlation for Sieve-Tray Point Efficiency, Entrainment, and Section Efficiency*", AIChE Journal, Vol. 43, No. 6, 1997, pp. 1611-1626.

[7] *ANSYS CFX 17.0 Documentation*, ANSYS Inc.

[8] Van Baten, J. M. and Krishna, R., "*Modelling Sieve Tray Hydraulics using Computational Fluid Dynamics*", Chemical Engineering Journal, Vol. 77, No. 3, 2000, pp. 143-151.

[9] Lieberman, N.P., and Lieberman, E.T., "*A Working Guide to Process Equipment*", McGraw-Hill, 4th Edition, 2014.

[10] Towler, G., and Sinnott, R.K., "*Chemical Engineering Design: Principles, Practice and Economics of Plant and Process Design*", Elsevier Ltd., 2nd Edition, 2013.

[11] Kister, H. Z., "*Distillation Design*", McGraw-Hill, 1992.

[12] Gesit, G., Nandakumar, K. and Chuang, K. T., "*CFD Modeling of Flow Patterns and Hydraulics of Commercial-Scale Sieve Trays*", AIChE Journal, Vol. 49, No. 4, 2003, pp. 910-924.